Journal of Sound and Vibration (1999) **225**(2), 307–325
Article No. jsvi.1999.2272, available online at http://www.idealibrary.com on IDEAL®

APPLICATION OF THE VARIABLE PROJECTION METHOD FOR UPDATING MODELS OF MECHANICAL SYSTEMS

U. PRELLS AND M. I. FRISWELL

Department of Mechanical Engineering, University of Wales Swansea, Singleton Park, Swansea, SA2 8PP, Wales

(*Received* 31 *July* 1998, *and in final form* 9 *March* 1999)

To update the parameters of a mathematical model of a mechanical system usually a cost function is minimised which consists of the difference between calculated and measured quantities. This paper deals with the special case where the forces are unknown. Instead of following the usual way of handling this type of updating problem by *assuming* a model for the forces, in this paper the variable projection method is applied to *estimate* the unknown forces in addition to the model parameters. Under certain conditions this two-fold inverse problem can be solved by eliminating the force from the parameter estimation process. The remaining equation to estimate the model parameters consists of the projection of the response data, where the associated projector depends on the model parameters. This application of the variable projection method is essentially an extension of the output residual method and leads to an estimation equation which is non-linear with respect to the model parameters. The variable projection method is introduced and investigated for two general types of unknown forces. Two theoretical examples, wind excitation of a tower and a rotary machine under unknown unbalance configuration, and the experimental case of a free–free steel beam tested by hammer excitation, are presented and discussed.

1. INTRODUCTION

The successful design, maintenance and monitoring of modern mechanical structures depends on the reliability of the underlying mathematical model. In general, the mathematical model *a priori* will not reflect the dynamic properties of the system with sufficient accuracy. Thus, the model has to be updated, which requires data from dynamic tests. To perform such tests is always costly and in some cases not feasible, mainly due to difficulties in measuring the excitations. Thus, an appealing approach is to use data due to the "natural" excitation of the system, such as

- wind excitation of towers and tall buildings,
- excitation of bridges by traffic,

0022-460X/99/320307 + 19 $30.00/0

- machines under work load,
- off-shore platforms subject to sea wave excitation.

The main drawback of using these data is that the excitation is generally unknown. One way to solve this problem is to assume an excitation, such as a stochastically based excitation of wind forces or sea wave motion. For many purposes, the involved deviations between the real and the modelled excitation have negligible influence on the result. However, for the purpose of model updating these deviations may lead to significant estimation errors, since the underlying inverse problem is generally ill-posed and therefore sensitive to these deviations. This paper investigates the possibilities of estimating the unknown forces in addition to the model parameters, using the variable projection method (VPM).

In the next section, the parameterization of a spatially discretized model in the frequency domain is introduced. The basic estimation equation of the output residual method (ORM) is recalled and extended to the case of unknown forces using the VPM. Modifications of the resulting estimation equation for two types of forces are investigated. The final section contains two academic simulation examples and an experimental example. The simulated examples are the damage detection of a tower subject to wind force with unknown excitation spectrum, and the foundation estimation of a rotor due to unknown unbalance configuration. The experimental example is a steel beam which has been hammer-tested in elastic slings with and without an added mass. The method has been applied to update a finite beam element model of the steel beam and to estimate the change in the mass matrix due to the added mass.

2. COMBINING OUTPUT RESIDUAL METHOD WITH VARIABLE PROJECTION METHOD

In this section, the parameterization of the mathematical model is introduced. The ORM is recalled briefly and is extended using the VPM. For two general types of unknown forces an estimation equation is derived, which leads to the definition of a cost function. This section concludes with some aspects concerning the ill-posedness of the resulting non-linear inverse problem.

2.1. PARAMETERIZATION OF THE MATHEMATICAL MODEL

The description of a spatially discretized mathematical model with n degree-of-freedom (d.o.f.) of a linear mechanical system in the frequency domain is given by the dynamic stiffness matrix at frequency $\omega \in \Omega \subset [0, \omega_{max}]$

$$\mathbf{F}(\omega) := -\omega^2 \mathbf{A}_2 + \mathrm{j}\omega \mathbf{A}_1 + \mathbf{A}_0 \in \mathbb{C}^{n \times n}, \tag{1}$$

which maps the response vector $\mathbf{u}(\omega)$ to the excitation vector $\mathbf{p}(\omega)$ that is

$$\mathbf{F}(\omega)\mathbf{u}(\omega) = \mathbf{p}(\omega) \in \mathbb{C}^n. \tag{2}$$

The model matrices $\mathbf{A}_i \in \mathbb{R}^{n \times n}$, $i = 0, 1, 2$, represent the contributions of stiffness, damping and inertia respectively. To update the uncertain model parts each matrix can be understood as a linear function

$$\mathbf{A}_i(\mathbf{q}_i) := \mathbf{A}_i^C + \sum_{r=1}^{n_i} \mathbf{A}_{ir} q_{ir} \in \mathbb{R}^{n \times n} \tag{3}$$

of dimensionless adjustment parameters $\mathbf{q}_i := (q_{i1}, \ldots, q_{in_i})^{\mathrm{T}} \in \mathbb{R}^{n_i}$ such that at $\mathbf{q}_i = (1, \ldots, 1)^{\mathrm{T}}$ the initial model results. The matrices $\mathbf{A}_{ir}$ are constant sparse matrices reflecting the substructures of the model, and the matrices $\mathbf{A}_i^C$ represent the *a priori* known model parts. For example, in the case of a finite element model, $\mathbf{A}_{01}$ may represent the contribution of the bending stiffness of the first beam element. Assembling all parameters in one vector $\mathbf{q} = (\mathbf{q}_0^{\mathrm{T}}, \mathbf{q}_1^{\mathrm{T}}, \mathbf{q}_2^{\mathrm{T}})^{\mathrm{T}} \in \mathbb{R}^{n_q}$ where $n_0 + n_1 + n_2 =: n_q$, the dynamic stiffness matrix becomes a function of the parameter vector $\mathbf{q}$. The restriction of the domain of $\mathbf{q}$ to the subset

$$\mathbb{S} := \{\mathbf{q} \in \mathbb{R}^{n_q} : \det[\mathbf{F}(\mathbf{q}, \omega)] \neq 0 \ \forall \omega \in \Omega\} \tag{4}$$

ensures the existence of the model response as a continuous function of $\mathbf{q}$

$$\mathbf{u}(\omega, \mathbf{q}) := \mathbf{F}^{-1}(\mathbf{q}, \omega)\mathbf{p}(\omega). \tag{5}$$

In general, $n_H \leqslant n$ components u_{i_l}, $l = 1, \ldots, n_H$ (sensor position), of the response vector and $n_S \leqslant n$ components f_{k_l}, $l = 1, \ldots, n_S$ (exciter positions), of the excitation vector will be available from dynamic tests. Introducing the selecting matrices

$$\mathbf{S}_o := [\mathbf{e}_{i_1}, \ldots, \mathbf{e}_{i_{n_S}}] \in \mathbb{R}^{n \times n_S}, \tag{6}$$

$$\mathbf{H}_o := [\mathbf{e}_{k_1}, \ldots, \mathbf{e}_{k_{n_H}}] \in \mathbb{R}^{n \times n_H}, \tag{7}$$

where $\mathbf{e}_k \in \mathbb{R}^n$ is the kth unit vector consisting of zeros except in the kth component, the available parts of the excitation and response vector are defined by

$$\mathbf{p}(\omega) := \mathbf{S}_o \mathbf{f}(\omega) \tag{8}$$

and

$$\tilde{\mathbf{u}}(\omega, \mathbf{q}) := \underbrace{\mathbf{H}_o^{\mathrm{T}} \mathbf{F}^{-1}(\mathbf{q}, \omega) \mathbf{S}_o}_{=: \mathbf{G}(\mathbf{q}, \omega)} \mathbf{f}(\omega). \tag{9}$$

Note, that other constraints can also be enforced, as for instance $q_\alpha > 0$, $\forall \alpha = 1, \ldots, n_q$, which guarantees the positive-definiteness of the model matrices.

2.2. THE OUTPUT RESIDUAL METHOD

Now the ORM is recalled briefly. An overview over different updating methods can be found in Friswell and Mottershead [1]. For a detailed discussion on various updating methods see, for instance, Natke *et al.* [2]. To fit the model to the data $\mathbf{u}^M(\omega) \in \mathbb{C}^{n_H}$, a parameter vector $\mathbf{q}$ has to be estimated which minimizes the distance between model response and measurements

$$\min_{q \in \mathbb{S}} \left\{ \sum_{i=1}^{m} \| \tilde{\mathbf{u}}(\omega_i, \mathbf{q}) - \mathbf{u}^M(\omega_i) \|^2 \right\}. \tag{10}$$

In case of the Euclidean norm $\|..\|$ the minimization problem (10) is equivalent to the non-linear inverse problem to estimate $\mathbf{q}$ that minimizes the equation error of

$$\mathbf{g} = \mathbf{B}(\mathbf{q})\mathbf{h}, \tag{11}$$

where the generalized output vector $\mathbf{g} \in \mathbb{R}^{2mn_H}$ and input vector $\mathbf{h} \in \mathbb{R}^{2mn_S}$ contain the real and imaginary parts of the measured response vector and the excitation vector respectively, for m frequencies, $w_i \in \Omega$, $i = 1, \ldots, m$, i.e.

$$\mathbf{g} = \begin{pmatrix} \mathrm{Re}\{\mathbf{v}\} \\ \mathrm{Im}\{\mathbf{v}\} \end{pmatrix}, \qquad \mathbf{h} = \begin{pmatrix} \mathrm{Re}\{\mathbf{r}\} \\ \mathrm{Im}\{\mathbf{r}\} \end{pmatrix}, \tag{12}$$

where the complex-valued vectors $\mathbf{v}$ and $\mathbf{r}$ are defined by

$$\mathbf{v} := \begin{pmatrix} \mathbf{u}^M(\omega_1) \\ \vdots \\ \mathbf{u}^M(\omega_m) \end{pmatrix}, \qquad \mathbf{r} := \begin{pmatrix} \mathbf{f}(\omega_1) \\ \vdots \\ \mathbf{f}(\omega_m) \end{pmatrix}. \tag{13}$$

The matrix $\mathbf{B}(\mathbf{q})$ has the form

$$\mathbf{B}(\mathbf{q}) = \begin{bmatrix} \mathrm{Re}\{\mathbf{X}(\mathbf{q})\} & -\mathrm{Im}\{\mathbf{X}(\mathbf{q})\} \\ \mathrm{Im}\{\mathbf{X}(\mathbf{q})\} & \mathrm{Re}\{\mathbf{X}(\mathbf{q})\} \end{bmatrix}, \tag{14}$$

with the block-diagonal matrix

$$\mathbf{X}(\mathbf{q}) := \begin{bmatrix} \mathbf{G}(\mathbf{q}, \omega_1) & & \mathbf{0} \\ & \ddots & \\ \mathbf{0} & & \mathbf{G}(\mathbf{q}, \omega_m) \end{bmatrix}. \tag{15}$$

Now the special case is investigated in which the force vector can be decomposed as

$$\mathbf{f}(\omega) = \mathbf{Z}(\omega)\mathbf{f}_o, \tag{16}$$

with the known excitation spectrum represented by $\mathbf{Z}(\omega) \in \mathbb{C}^{n_S \times n_S}$ and the unknown exciter configuration $\mathbf{f}_o \in \mathbb{R}^{n_S}$. The basic equation (11) becomes

$$\mathbf{g} = \mathbf{B}(\mathbf{q})\mathbf{f}_o, \tag{17}$$

where $\mathbf{B}(\mathbf{q}) \in \mathbb{R}^{2mn_H \times n_S}$ is now given by

$$\mathbf{B}(\mathbf{q}) = \begin{bmatrix} \mathrm{Re}\{\mathbf{X}(\mathbf{q})\} \\ \mathrm{Im}\{\mathbf{X}(\mathbf{q})\} \end{bmatrix} \tag{18}$$

and the complex-valued matrix $\mathbf{X}(\mathbf{q})$ is defined as

$$\mathbf{X}(\mathbf{q}) := \begin{bmatrix} \mathbf{G}(\mathbf{q}, \omega_1)\mathbf{Z}(\omega_1) \\ \vdots \\ \mathbf{G}(\mathbf{q}, \omega_m)\mathbf{Z}(\omega_m) \end{bmatrix} \tag{19}$$

2.3. THE VARIABLE PROJECTION METHOD

In this section, the VPM is linked to the output-residual-based estimation equation. The VPM is introduced briefly. For further reading see, for instance, Golub and Pereyra [3].

For both types of unknown forces the following derivation is formally the same. Thus, let $\mathbf{y}$ be either $\mathbf{h}$ (first case, equation (11)) or $\mathbf{f}_o$ (second case, equation (17)) and consider the estimation equation

$$\mathbf{B}(\mathbf{q})\mathbf{y} = \mathbf{g}. \tag{20}$$

If it is assumed that the parameter vector $\mathbf{q}$ is given, equation (20) can be solved in the least-squares sense for $\mathbf{y}$,

$$\bar{\mathbf{y}} = \mathbf{B}^+(\mathbf{q})\mathbf{g}. \tag{21}$$

Here the superscript $+$ denotes the Moore–Penrose inverse (see, for instance, Boullion and Odell [4]). Inserting this result into equation (20) the relative quadratic equation error becomes

$$e_R(\mathbf{q}) := \|\mathbf{g} - \mathbf{B}(\mathbf{q})\mathbf{B}^+(\mathbf{q})\mathbf{g}\|^2/\|\mathbf{g}\|^2 \tag{22}$$

$$= \|[\mathbf{I}_{2mn_H} - \mathbf{P}(\mathbf{q})]\mathbf{g}\|^2/\|\mathbf{g}\|^2 \tag{23}$$

$$= \|\mathbf{N}(\mathbf{q})\mathbf{g}\|^2/\|\mathbf{g}\|^2 \tag{24}$$

$$= 1 - \mathbf{g}^{\mathrm{T}}\mathbf{P}(\mathbf{q})\mathbf{g}/\|\mathbf{g}\|^2, \tag{25}$$

where $\mathbf{P}(\mathbf{q}) := \mathbf{B}(\mathbf{q})\mathbf{B}^+(\mathbf{q})$ is the projector into the subspace spanned by the columns of $\mathbf{B}(\mathbf{q})$, and $\mathbf{N}(\mathbf{q}) := \mathbf{I}_{2mn_H} - \mathbf{P}(\mathbf{q})$ is the projector into the orthogonal complement. Note that $0 \leqslant e_R(\mathbf{q}) \leqslant 1$, because of the orthonormal decomposition

$$\mathbf{g}/\|\mathbf{g}\| = \mathbf{N}(\mathbf{q})\mathbf{g}/\|\mathbf{g}\| + \mathbf{P}(\mathbf{q})\mathbf{g}/\|\mathbf{g}\|. \tag{26}$$

Equation (25) represents a non-linear inverse problem to be solved for $\mathbf{q}$,

$$\min_{q \in \mathbb{S}} \{e_R(\mathbf{q})\}, \tag{27}$$

which is independent of the unknown excitation. If a parameter vector has been estimated, equation (21) is an estimate of the force. In the first case the projectors are not trivial, i.e. $\mathbf{P} \neq \mathbf{I}_{2mn_H}$, $\mathbf{N} \neq \mathbf{0}$, if $n_H > n_S$. In the second case the projectors are not trivial if $2mn_H > n_S$.

Remark. A common solution method of equation (27), as for instance discussed in Kaufman [5], assumes differentiability† of the projector, which is numerically related to the singular values of $\mathbf{B}(\mathbf{q})$, and which, since in general $\mathbf{B}(\mathbf{q})$ is ill-conditioned, is difficult to decide and to monitor during the iterative solution procedure. Like all parametric model estimation methods the condition is closely related the number of modes contained in the frequency range Ω. Numerically, the

† A sufficient condition is $\mathrm{rank}[\mathbf{B}(\mathbf{q})] = \text{constant}$.

decision of the rank of $\mathbf{B}(\mathbf{q})$ is usually made by considering its singular values. It is well known that the contribution of the small singular values of $\mathbf{B}(\mathbf{q})$ can amplify the effect of data errors in $\mathbf{g}$ on the estimate $\bar{\mathbf{y}}$. The use of a positive-definite weighting matrix $\mathbf{W} = \mathbf{V}^T\mathbf{V}$, which can be introduced formally by substituting $\mathbf{g}$ by $\mathbf{Vg}$ and $\mathbf{B}(\mathbf{q})$ by $\mathbf{VB}(\mathbf{q})$, can minimize the effect of the data errors on the estimates; in general, however, further regularization is necessary to obtain unique and stable solutions. Since the introduction of regularization methods is beyond the scope of this paper, no noise was considered in the simulation examples, and for the test case of a free–free beam only an output weighing matrix has been used for regularization.

3. EXAMPLES

The next two examples are simulation studies to clarify the theoretical approach introduced in the preceding section. The final example is a real test case.

3.1. DAMAGE DETECTION OF A FIVE-STOREY STRUCTURE SUBJECT TO WIND EXCITATION

The following example stems from Andersen [6]. A model of a tower will be considered in which only the horizontal displacement at each of the five floors is assumed non-zero, i.e. $n = 5$. The masses are assumed to be concentrated in the centre of each storey. The first d.o.f. corresponds to the top of the tower (fifth floor). The entire model is scaled such that the mass matrix is the unit matrix $\mathbf{A}_2 = \mathbf{I}_5$. The damping and stiffness matrices are given by

$$\mathbf{A}_1 = \begin{bmatrix} 2{\cdot}41 & -2{\cdot}4 & 0 & 0 & 0 \\ -2{\cdot}4 & 4{\cdot}81 & -2{\cdot}4 & 0 & 0 \\ 0 & -2{\cdot}4 & 4{\cdot}81 & -2{\cdot}4 & 0 \\ 0 & 0 & -2{\cdot}4 & 4{\cdot}81 & -2{\cdot}4 \\ 0 & 0 & 0 & -2{\cdot}4 & 3{\cdot}01 \end{bmatrix}, \tag{28}$$

$$\mathbf{A}_0 = \begin{bmatrix} 4800 & -4800 & 0 & 0 & 0 \\ -4800 & 9600 & -4800 & 0 & 0 \\ 0 & -4800 & 9600 & -4800 & 0 \\ 0 & 0 & -4800 & 9600 & -4800 \\ 0 & 0 & 0 & -4800 & 6000 \end{bmatrix}. \tag{29}$$

The problem is to detect damage using responses due to wind excitation. The damage is modelled by a horizontal stiffness loss between the first and second storey, which is already incorporated into the definition of $\mathbf{A}_0$. The stiffness between the first and second storey is 4800 N/m. Referring to the parameterization introduced in Section 2.1 the damage detection is equivalent to the estimation of the positive adjustment parameter **q** of the stiffness matrix

$$\mathbf{A}_0(q) = \mathbf{A}_0^c + q \begin{bmatrix} 0 & 0 & 0 & 0 & 0 \\ 0 & 0 & 0 & 0 & 0 \\ 0 & 0 & 0 & 0 & 0 \\ 0 & 0 & 0 & 4800 & -4800 \\ 0 & 0 & 0 & -4800 & 4800 \end{bmatrix}, \tag{30}$$

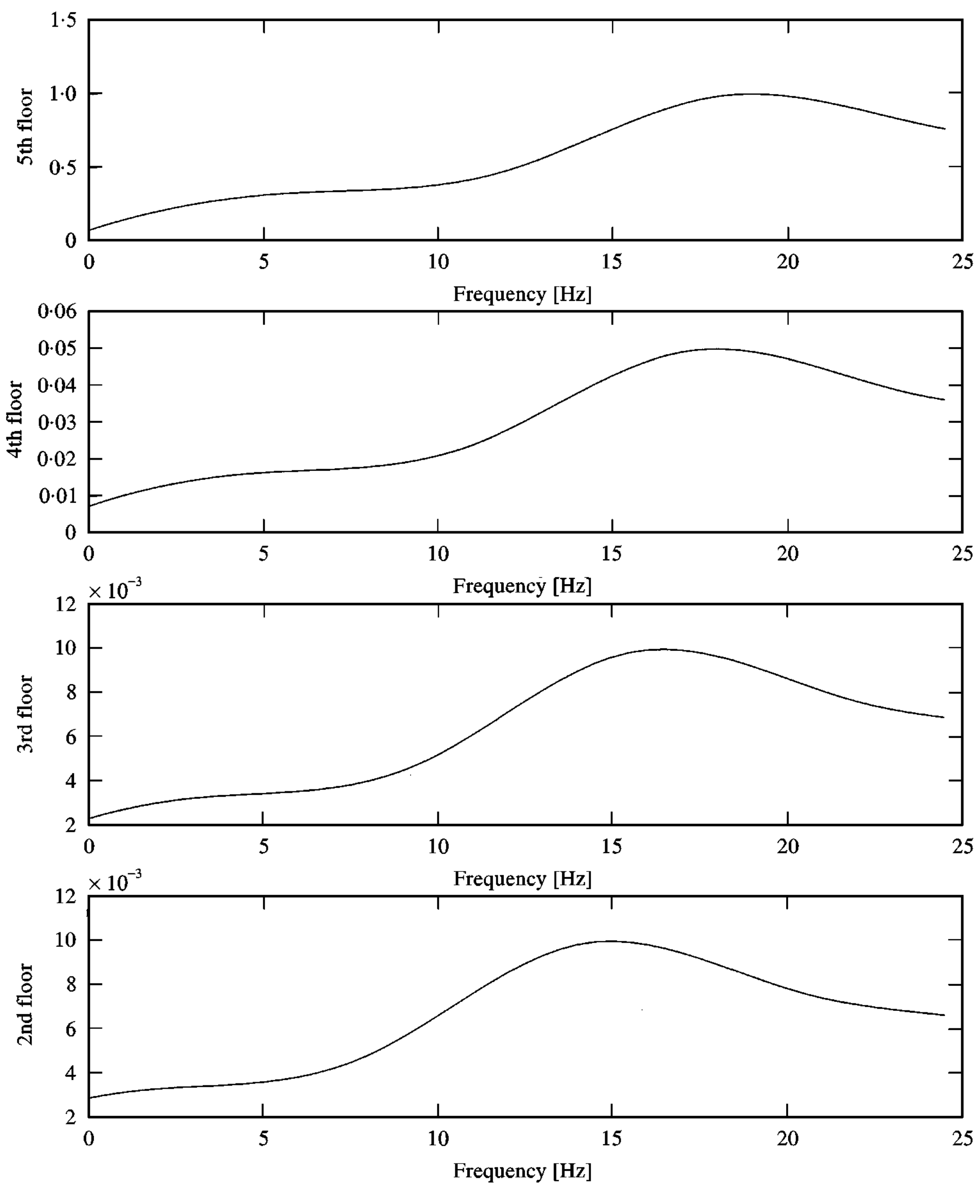

Figure 1. Simulated wind force spectrum.

where the 'true' parameter value $\mathbf{q} = 1$. To simulate the wind excitation the spectrum of the forces depicted in Figure 1 are assumed, which covers the eigenfrequencies 2·14, 7·59, 13·29, 17·97, 20·99 Hz. The force at the top of the tower (first d.o.f.) is the largest because a plate has been attached there to increase the wind force. The force at the first floor is assumed to be zero. To complete the test simulation the responses due to this excitation are assumed to be measured at the fifth, at the third and at the first storey (see Figure 2) with $m = 50$ frequencies covering a spectrum $\Omega = 2\pi[0, 24{\cdot}5]$ rad/s. The selecting matrix of the response is given by $\mathbf{H}_o = [\mathbf{e}_1, \mathbf{e}_3, \mathbf{e}_5]$. Thus, the matrix $\mathbf{B}(\mathbf{q})$ defined in equation (14) has $2mn_h = 2 \cdot 50 \cdot 3 = 300$ rows. To evaluate the number of columns of $\mathbf{B}(\mathbf{q})$ the selecting matrix of the excitation has to be defined. For the purpose of simulating the response data, the selecting matrix was chosen to be $\mathbf{S}_o = [\mathbf{e}_1, \mathbf{e}_2, \mathbf{e}_3, \mathbf{e}_4]$. However, it is known that due to the attached plate the wind excites mainly the top of the tower. Thus, neglecting the wind force at all other d.o.f. one finds that with

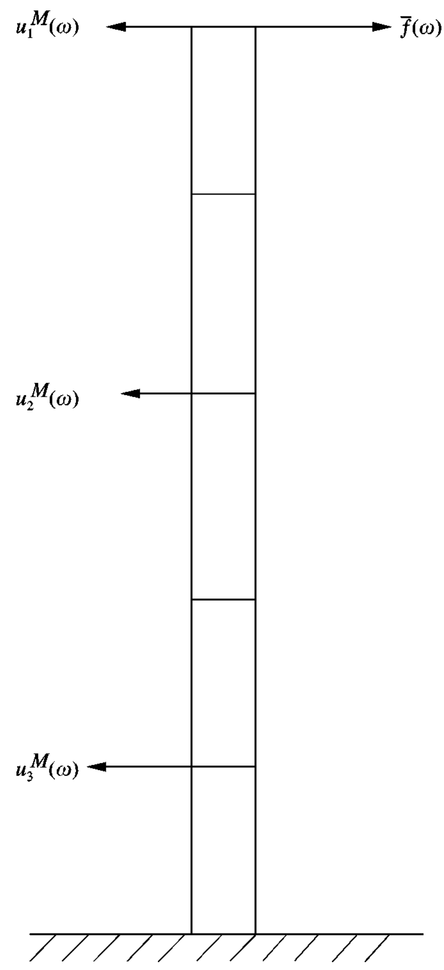

Figure 2. Model of a five-storey tower.

reference to Section 2.2

$$\mathbf{S}_o = \mathbf{e}_1, \tag{31}$$

and therefore the matrix $\mathbf{B}(q)$ has the format 300×100.

In Figure 3 the relative error $e_R(q)$ defined in equation (25) is plotted for parameter values $q \in [0{\cdot}5, 1{\cdot}5]$. The minimum value is obvious. It can now be used to estimate the wind force. In Figure 4 the wind force at the first d.o.f. and the estimated force using equation (21) are depicted. Although the assumed selecting matrix (31) was not correct, the fit is acceptable. The deviation in the upper spectrum is due to the poor excitation of the fifth mode corresponding to an eigenfrequency of about 21 Hz. This completes the example of the case in which the spectrum of the force is unknown. In the next section an example is presented where the frequency dependence of the force is known, but the location and magnitudes are unknown.

3.2. ESTIMATION OF A FOUNDATION MODEL OF A ROTARY MACHINE

The rotor is simulated by an Euler–Bernoulli beam (see Figure 5) which is spatially discretized using four beam elements. The length of the beam is 2·3 m, the diameter is 0·1 m, the density is 7850 kg/m^3, and Young's modulus is $2{\cdot}1 \times 10^{11}$ N/m^2. Each beam element is defined by two nodes. Each node has two d.o.f: one translational and one rotational. Thus the dimension of the beam model

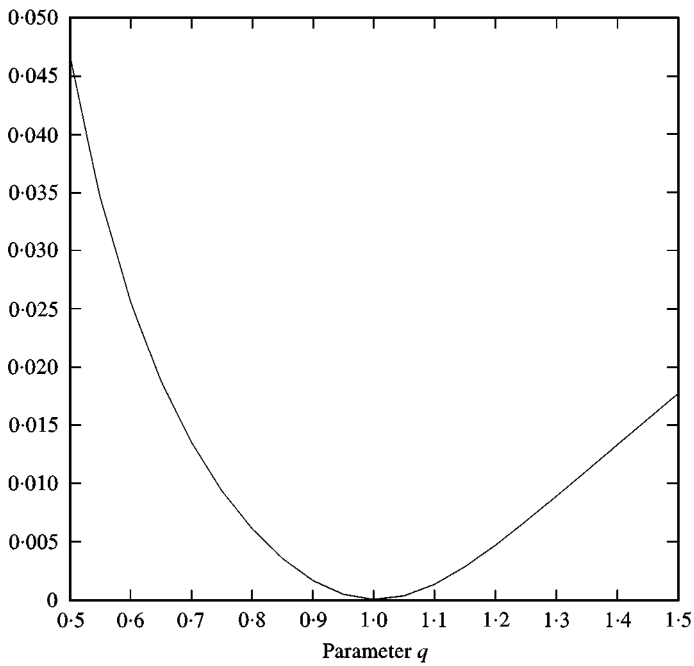

Figure 3. Relative quadratic equation error e_R.

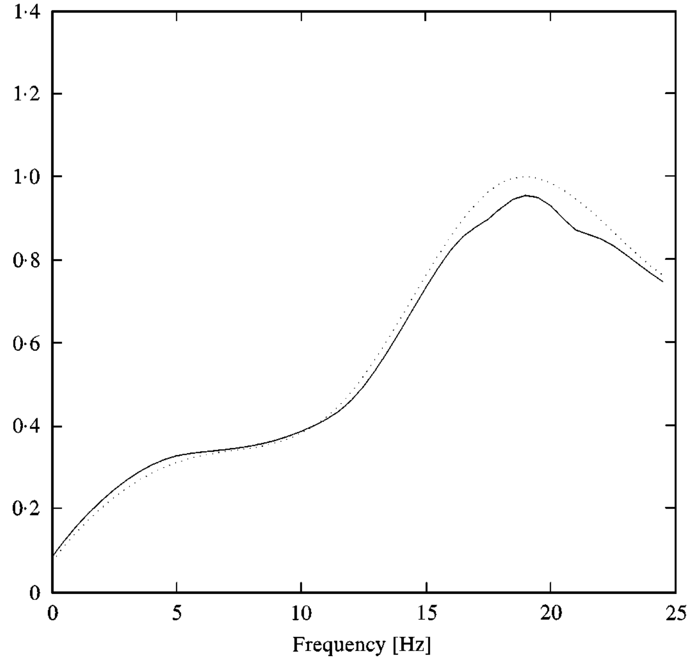

Figure 4. Simulated (dotted) and estimated (solid) wind force at fifth floor.

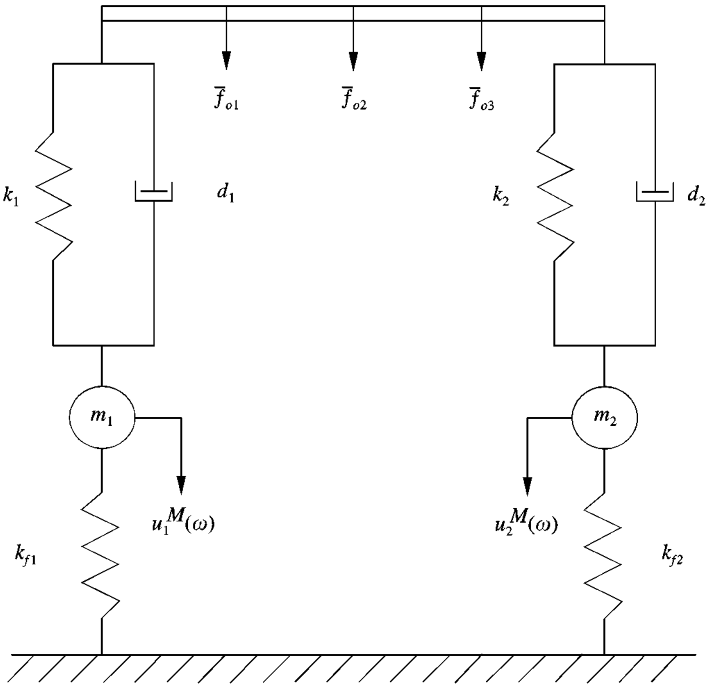

Figure 5. Model of a rotor mounted on a foundation via journal bearings.

is 10. The first and the last node of the rotor model is viscoelastically connected to a foundation. The viscoelastic interface represents the oil film of journal bearings which are, for the sake of simplicity, modelled by two massless springs with stiffnesses $k_1 = 1{\cdot}77 \times 10^8$ and $k_2 = 3{\cdot}54 \times 10^8$ N/m, and by two dampers with $d_1 = d_2 = 5 \times 10^7$ Ns/m respectively. The foundation is modelled by an unconnected pair of masses $m_1 = 90$, $m_2 = 135$ kg and springs with stiffnesses $k_{f1} = k_{f2} = 1{\cdot}77 \times 10^7$ N/m. Thus, the dimension of the entire model is $n = 12$. It is assumed that the responses are measured at the d.o.f. of the two masses m_1, m_2 during a slow rundown of the machine, covering the frequency range $\Omega = 2\pi[0{\cdot}5, 100]$ rad/s with equally spaced steps of 0·5 Hz. Thus, $m = 200$ and $n_H = 2$, and with reference to Section 2.3 the matrix $\mathbf{B}(\mathbf{q})$ has $2mn_H = 2 \cdot 200 \cdot 2 = 800$ rows. To evaluate the number of columns of $\mathbf{B}(\mathbf{q})$ the selecting matrix of the excitation has to be defined. It is well known that in this case the unbalance force is given by (see equation (16) for $\mathbf{Z}(\omega) = \omega^2 \mathbf{I}_5$)

$$\mathbf{f}(\omega) = \omega^2 \mathbf{f}_o, \tag{32}$$

where the real-valued configuration vector $\mathbf{f}_o$ contains the unbalance masses and eccentricities, which are assumed to be unknown. For simulation purposes it is assumed that there exists a continuous unbalance distribution along the rotor, discretely modelled by

$$\mathbf{f}_o = (0{\cdot}005, 0{\cdot}01, 0{\cdot}1, 0{\cdot}05, 0{\cdot}02)^{\mathrm{T}} \tag{33}$$

with the selecting matrix $\mathbf{S}_o = [\mathbf{e}_1, \mathbf{e}_3, \mathbf{e}_5, \mathbf{e}_7, \mathbf{e}_9]$ which correspond to the translational d.o.f. of the rotor. In Figure 6 the responses at the two d.o.f. are shown. Since there are three resonances in the rundown range the problem will be restricted to the estimation of the unbalances at three balance planes given by the selecting matrix

$$\mathbf{S}_o = [\mathbf{e}_3, \mathbf{e}_5, \mathbf{e}_7] \tag{34}$$

and to the estimation of the foundation stiffnesses k_{f1}, k_{f2} using the parameterization

$$\begin{pmatrix} k_{f1} \\ k_{f2} \end{pmatrix} \to \begin{pmatrix} q_1 k_{f1} \\ q_2 k_{f2} \end{pmatrix}, \tag{35}$$

where the ‘true’ parameter vector is $\mathbf{q} = (1, 1)^{\mathrm{T}}$. Thus, the matrix $\mathbf{B}(\mathbf{q})$ has the format 800×3.

In Figure 7 the surface of the relative quadratic equation error $e_R(\mathbf{q})$ is plotted over the plane $\mathbf{q} \in [0{\cdot}8, 1{\cdot}2]^2$. Although there are some local minima the surface shows a unique global minimum at the ‘true’ parameter values. Using these values to estimate the configuration vector $\mathbf{f}_o$ leads to

$$\bar{\mathbf{f}}_o = \mathbf{B}^+(\mathbf{q})\mathbf{g} = \begin{pmatrix} 0{\cdot}0383 \\ 0{\cdot}0422 \\ 0{\cdot}1036 \end{pmatrix}. \tag{36}$$

In order to verify whether the estimated unbalance configuration is sufficient to reproduce the data, the model responses have been calculated using $\bar{\mathbf{f}}_o$. The error

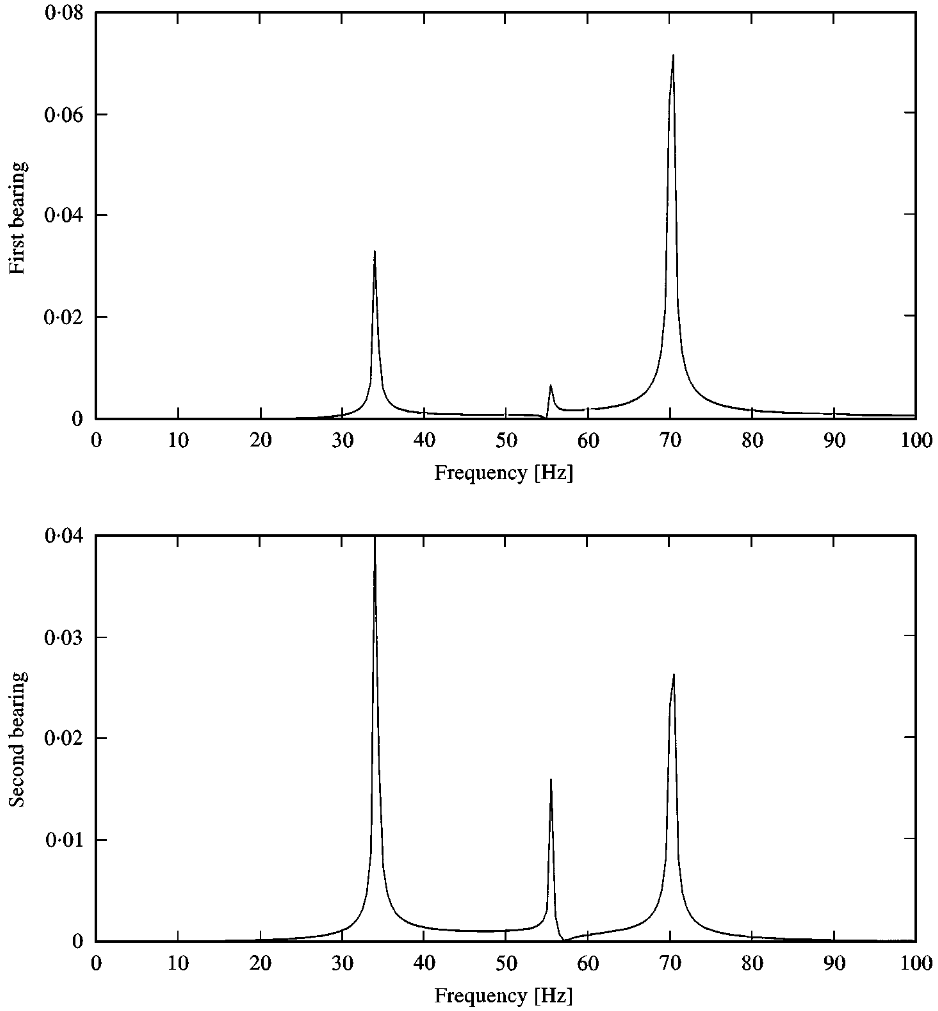

Figure 6. Simulated responses.

magnitude between the simulated and the model responses are shown in Figure 8. Although the error has local maxima at the resonances and increases with the frequency the overall fit is satisfactory.

Remark. Since there are only three resonances in the rundown range the unbalance vectors $\mathbf{f}_o$ and $\bar{\mathbf{f}}_o$ are equivalent.

3.3. MODEL ESTIMATION A STEEL BEAM TESTED BY HAMMER EXCITATION

A steel beam (see Figure 9) of size $0{\cdot}0062\,\text{m} \times 0{\cdot}025\,\text{m} \times 0{\cdot}856\,\text{m}$ (thickness × height × length), Young's modulus $2{\cdot}07 \times 10^{11}\,\text{N/m}^2$ and density

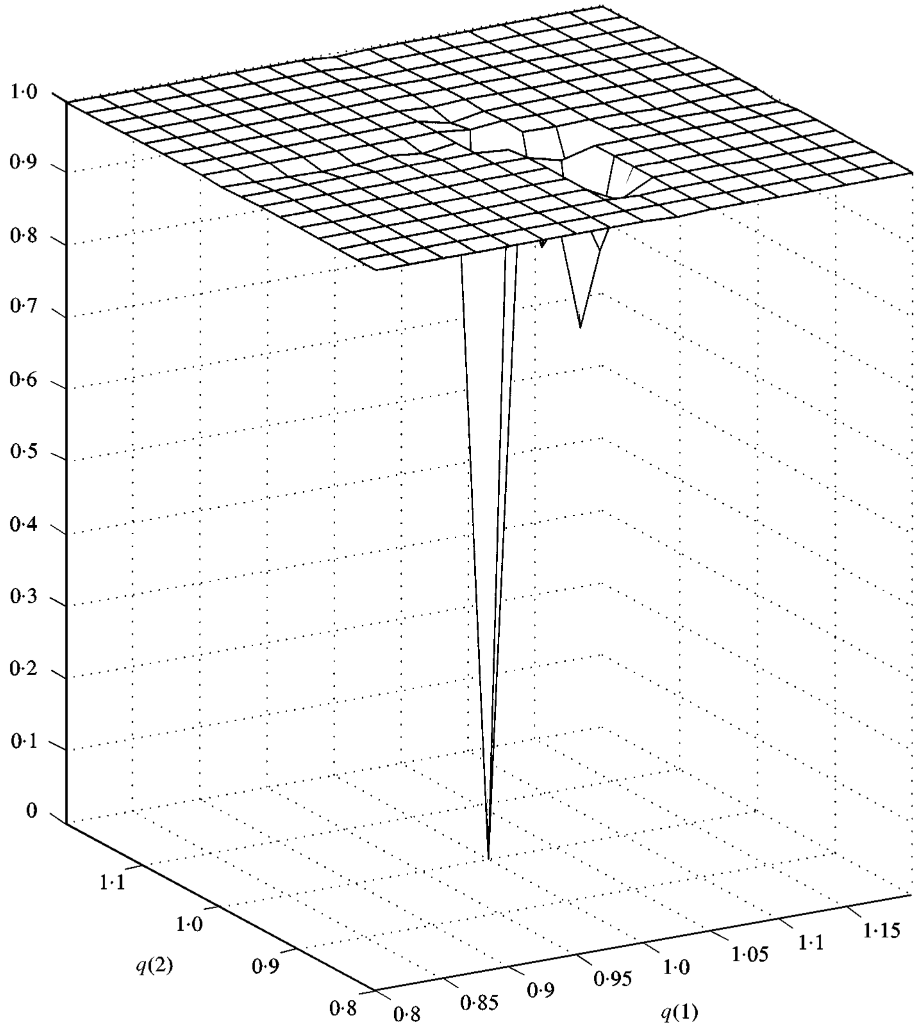

Figure 7. Surfaces of relative quadratic error $e_R(\mathbf{q})$.

7800 kg/m^3 was supported in elastic slings. Five piezo-electric accelerometers were attached to the beam at positions r_1, r_2, r_4, r_6 and r_7. The beam was excited using an intrumented hammer at position r_5. Using $m = 1281$ equally spaced frequencies within the range between 100 and 900 Hz the responses $\mathbf{u}_O^M(\omega) \in \mathbb{C}^5$ show five distinct resonances at 123·0, 240·9, 402·4, 597·1 and at 832·8 Hz. The hammer test was repeated with an additional mass of 33 g magnetically attached at position r_6. Compared with data $\mathbf{u}_O^M$ (beam without added mass), data $\mathbf{u}_A^M$ (beam with added mass) show a distinct shift in the resonances. From both sets of data, an output weighting matrix has been derived in order to reduce the effect of data noise to the estimates. A finite beam element model was reduced to order $n = 7$ using the modal contributions of the five resonances of the response and two additional model resonances 62·9 and 962·2 Hz, just outside the frequency range. The seven-d.o.f. of

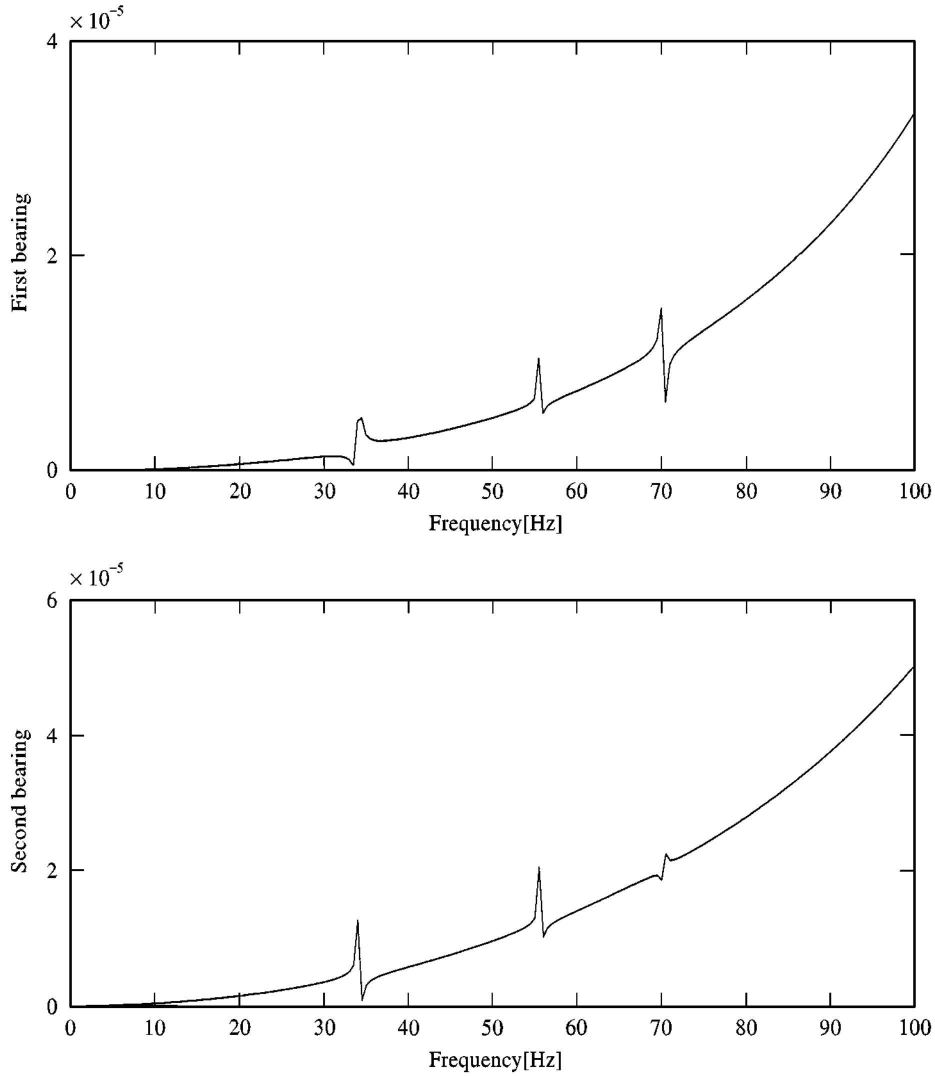

Figure 8. Error between simulated and model response.

the reduced model correspond to the positions r_1–r_7 (see Figure 9). Thus, the output selecting matrix is

$$\mathbf{H}_o = [\mathbf{e}_1, \mathbf{e}_2, \mathbf{e}_4, \mathbf{e}_6, \mathbf{e}_7], \tag{37}$$

and the selecting matrix of the ecitation is

$$\mathbf{S}_o = \mathbf{e}_5. \tag{38}$$

Two estimation problems have been studied:

P1 Estimation of a damping matrix and update of the mass and stiffness matrices of the modal reduced model of the steel beam to fit the data $\mathbf{u}_O^M$.

P2 Updating of the mass matrix of the model resulting from P1 to fit the data $\mathbf{u}_A^M$.

For the case P1, the number of model parameters is $n_q = 3 \cdot 7 \cdot (7+1)/2 = 84$ which corresponds to the number of independent elements of the three symmetric 7×7 matrices $\mathbf{A}_0$, $\mathbf{A}_1$, $\mathbf{A}_2$. In case P2, the estimation of a change $\Delta\mathbf{A}_2$ of the mass matrix

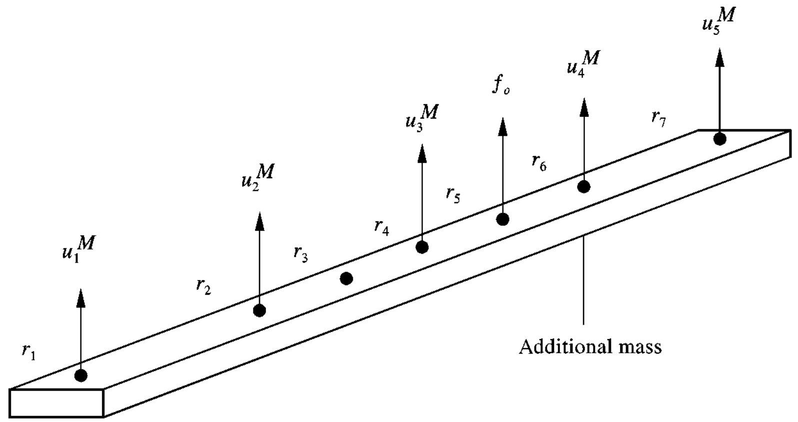

Figure 9. Hammer test of a free–free steel beam: f_o location of excitation, u_i^M measured responses.

TABLE 1

Estimation results

		P1		P2	
	Model Data	Reduced $\mathbf{u}_O^M$	Updated $\mathbf{u}_O^M$	Updated $\mathbf{u}_A^M$	Updated mass $\mathbf{u}_A^M$
S1	$e_R =$	0·0012	$1{\cdot}46 \times 10^{-4}$	0·0034	0·0013
	$\bar{f}(\omega)$ see Figure 11:	left top	right top	left bottom	right bottom
S2	$e_R =$	0·2432	$1{\cdot}77 \times 10^{-4}$	0·3474	0·0073
	$\bar{\mathbf{f}}_o =$	$\begin{pmatrix} -0{\cdot}63 \\ -2{\cdot}38 \\ 1{\cdot}45 \\ -2{\cdot}86 \\ 0{\cdot}86 \\ -2{\cdot}34 \\ -1{\cdot}15 \end{pmatrix}$	$\begin{pmatrix} -0{\cdot}002 \\ -0{\cdot}010 \\ 0{\cdot}001 \\ -0{\cdot}011 \\ 1{\cdot}001 \\ -0{\cdot}010 \\ -0{\cdot}002 \end{pmatrix}$	$\begin{pmatrix} -0{\cdot}79 \\ -2{\cdot}68 \\ 1{\cdot}18 \\ -3{\cdot}05 \\ 1{\cdot}06 \\ -2{\cdot}53 \\ -0{\cdot}91 \end{pmatrix}$	$\begin{pmatrix} -0{\cdot}12 \\ -0{\cdot}24 \\ 0{\cdot}16 \\ -0{\cdot}29 \\ 1{\cdot}19 \\ -0{\cdot}19 \\ -0{\cdot}06 \end{pmatrix}$

requires parameter vector $\mathbf{q} \in \mathbb{R}^{28}$. For each problem, two scenarios have been studied corresponding to the general types of unknown forces (see Section 2.3):

S1 The exciter position $\mathbf{S}_o = \mathbf{e}_5$ is known but the spectrum of the excitation $f(\omega) = 1$ is unknown.
S2 The spectrum of the excitation $\mathbf{Z}(\omega) = \mathbf{I}_7 = \mathbf{S}_o$ is known but the exciter position $\mathbf{f}_o = \mathbf{e}_5 \in \mathbb{R}^7$ is unknown.

In the first case (S1), the vector $\bar{\mathbf{h}}$ of force spectrum estimate has dimension $2 \cdot m = 2562$. In case S2 the vector $\bar{\mathbf{f}}_o$ of the force location estimate is seven-dimensional. An overview of the estimation results is given in Table 1 for the two problem formulations (P1 left-half, P2 right-half) and for each scenario (S1 upper-half, S2 lower-half). The force spectrum estimates are shown in Figure 10. Compared to S2 the errors e_R of scenario S1 are already small at the initial model. Because the number of columns of $\mathbf{B}$ is much larger (2562 in contrast to 7) the main part of the data vectors are already contained in the spanned subspaces. The

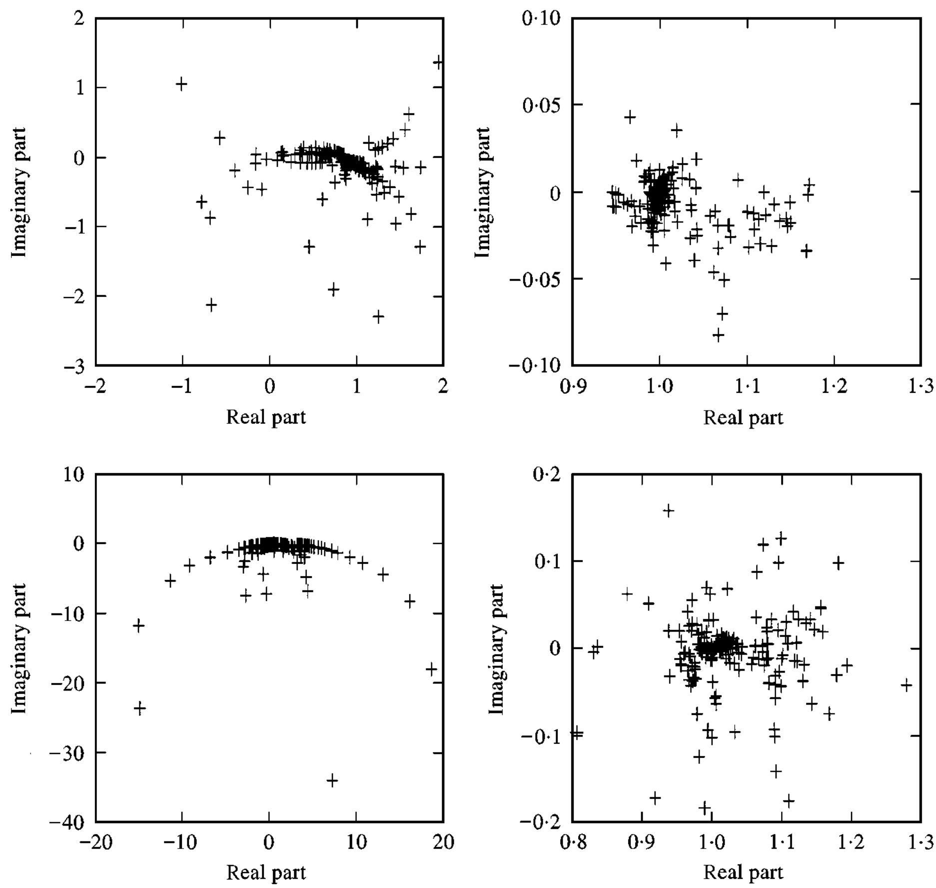

Figure 10. Phase plane force spectrum estimates using: modal reduced model and data set $\mathbf{u}_O^M$ (left top), updated model to fit $\mathbf{u}_O^M$ (right top), updated model and data set $\mathbf{u}_A^M$ (left bottom) and model with updated mass matrix to fit $\mathbf{u}_A^M$ (right bottom).

corresponding force spectrum estimates (left-half of Figure 10) reveal that the linear combinations that generate the data vector shows large deviations from the 'true' spectrum, which would correspond to the single point (1, 0) in the phase plane. In all cases the force estimates of the updated models are satisfactory. The force location estimates (second and last columns of the last row in Table 1) show only small deviations of the 'true' location $\mathbf{e}_6$. In contrast to the good fit of the force location estimates the estimation error of the force spectrum estimates is larger (right-half of Figure 10). At most frequencies the forces spectrum estimates are near the point (1, 0). However, there are a few relatively large errors at some frequencies. The estimates of the change of the mass matrix (problem P2) are almost identical for both scenarios. For scenario S2, the elements of the estimate $\overline{\Delta \mathbf{A}_2}$ are depicted in Figure 11. It clearly indicates that the main change of mass corresponds to a single mass of 43 g at position r_6 on the beam. Although the position has been estimated correctly the mass is overestimated. Using the model and the force estimates the corresponding model responses can be calculated. For both scenarios the

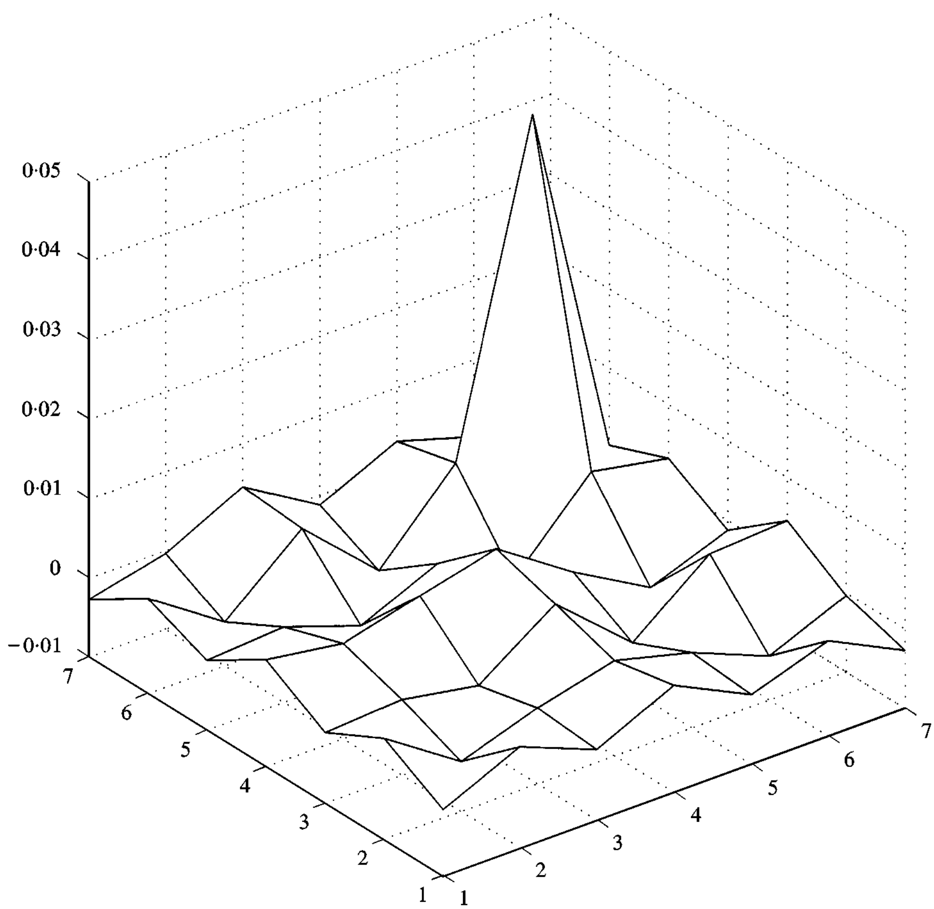

Figure 11. Components of the estimated change of the mass matrix.

calculated responses match the data well. In Figures 12, for example, the calculated (solid) and measured (dotted) displacements are shown for the scenario S1. The plots in the upper-half show the displacement at position r_5 near the first resonance (worst fit). In the lower-half the displacement at position r_1 is shown near the fifth resonance (best fit). Although the magnitudes of the model displacements are too low, the resonance frequencies match exactly.

Remark. During the estimation process several local minima have been found. Especially in case of scenario S1 (unknown force spectrum), the programme to minimize e_R had to be restarted for different initial parameter vectors. It appears that the increase of the dimension of the column space of $\mathbf{B}(q)$ increases the risk of finding local minima of similar low values e_R. To overcome the resulting non-uniqueness of the estimates regularization methods have to be applied.

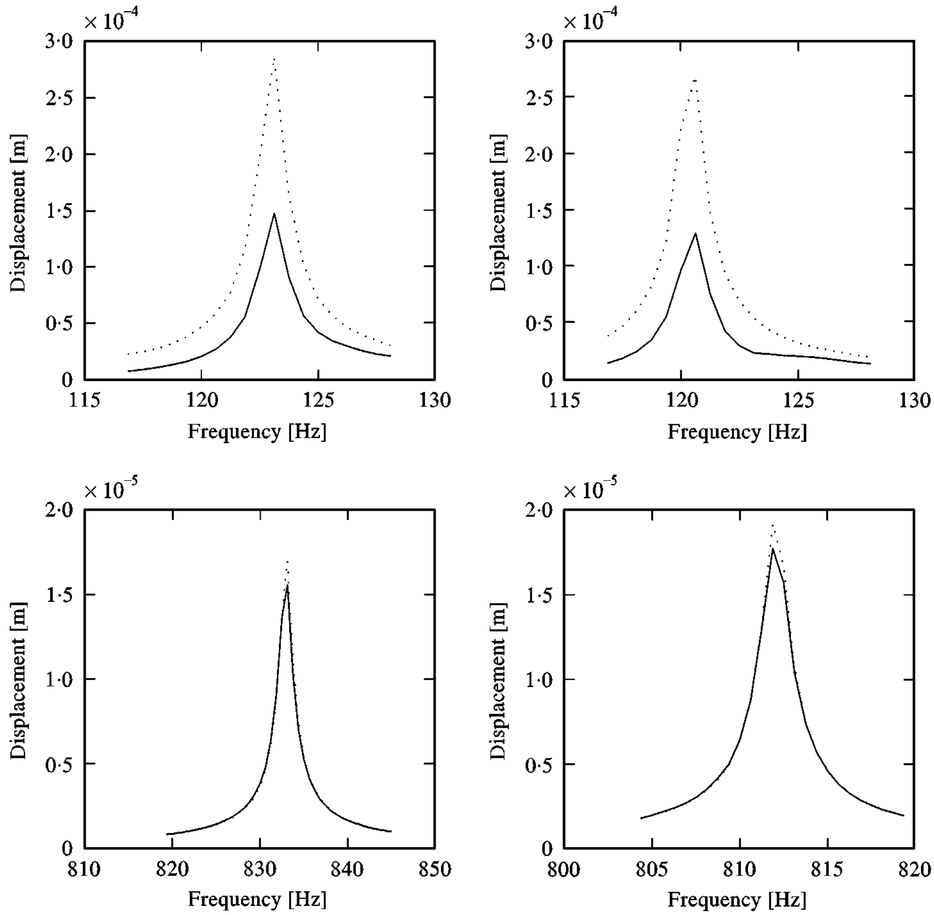

Figure 12. Scenario S1: calculated (solid) and measured (dashed) displacements near the first resonance at position r_5 (upper-half) and near the fifth resonance at position r_1 (lower-half) for problem P1 (left-half) and P2 (right-half).

4. CONCLUSION

This paper has extended the output residual method for updating finite element models of mechanical systems in the frequency domain to account for unknown forces. The VPM has been used to separate the estimation of the unknown model and the estimation of the unknown excitation. Although the VPM can deal with general unknown forces, incorporating knowledge of the forcing spectrum or location results in a considerable improvement in the quality of the estimated parameters. This was demonstrated in the examples. The first example showed that by assuming a known location for the dominant wind excitation of a five-storey tower, the force spectrum could be recovered to an acceptable accuracy. The second example of a rotor, excited by unbalance forces, showed that the distribution of the unbalance could be recovered because the spectrum of the excitation was known. Finally, the method was applied to update the model of a steel beam, which was dynamically tested by hammer excitation. Although the case of unknown force spectrum appears to be less stable than the case of unknown force location both estimation results were satisfactory. The application of the VPM to incorporate incomplete knowledge of the excitation forces has shown great promise. Further studies will concentrate on incorporating regularization into the method, and applying the method to industrial-scale problems.

REFERENCES

1. M. I. Friswell and J. E. Mottershead 1995 *Finite Element Model Updating in Structural Dynamics*. Dordrecht: Kluwer Academic Publisher.
2. H. G. Natke, G. Lallement, N. Cottin and U. Prells 1995 *Inverse Problems in Engineering*, **1**, 329–348. Properties for various residuals within updating of mathematical models.
3. G. H. Golub and V. Pereyra 1973 *SIAM Journal of Numerical Analysis*, 413–432. The differentiation of pseudo-inverses and nonlinear least squares probles whose variables separate.
4. T. Boullion and P. Odell 1974 *Generalized Inverse Matrices*. New York: Wiley.
5. L. Kaufman 1975 *BIT* 49–47. Variable projection method for solving separable nonlinear least squares problems.
6. P. Andersen 1997 *Ph.D. Thesis*, *Department of Building Technology and Structural Engineering*, *Aalborg University*. Identification of civil engineering structures using vector ARMA models.